# Numerical Study of I-Joists with Wood-Based Corrugated Panel Web

Abdessamad Jiloul [a,b,]* Pierre Blanchet [a,b] and Clément Boudaud [c]

Oriented strand board (OSB) panels are widely used as the best web solution for wooden I-joists. Many previous studies have focused on testing various new web materials, but few have examined the contribution of other web shapes to the I-joists' behavior. The use of corrugated wood-based panels as I-joist web has been investigated. The aim of this study was to analyze the sensitivity of the joist in bending tests to the elastic properties of the corrugated web using a numerical approach with the finite element method. Joists with a corrugated web were manufactured and tested in long- and short-span bending tests and compared to traditional I-joists with an OSB web. The results obtained were encouraging. Results show that the in-plane shear modulus is the most critical elastic property in the behavior of the joist and is estimated at 1300 MPa to reproduce the same behavior of the corrugated web joist as that experimentally tested. The numerical approach also enabled determination of the corrugated web's shear failure mode. This mode of failure manifested itself as interactive buckling, followed by the creation of diagonal tension lines.

*DOI: 10.15376/biores.20.1.737-764*

*Keywords: Corrugated panel web; OSB web; Wood I-joist; Bending and shear capacity; Finite element numerical modeling; Interactive buckling*

*Contact information: a: NSERC Industrial Chair on Eco-responsible Wood Construction, Université Laval, 2425 rue de la Terrasse, Quebec G1V 0A6, Canada; b: Renewable Materials Research Centre, Université Laval, 2425 rue de la Terrasse, Quebec G1V 0A6, Canada; c: LIMBHA, Ecole Supérieure du Bois et des Biosourcés (ESB), 7 Rue Christian Pauc, 44000 Nantes, France;*
** Corresponding author: abdessamad.jiloul.1@ulaval.ca*

## INTRODUCTION

In recent years, the use of wood as a building material has attracted particular and growing interest worldwide. The development of engineered wood-based products has encouraged this return to the wood material. These include wooden I-joists, which are increasingly used as roof and floor joists in commercial and residential construction. Wooden I-joists are an effective alternative to solid sawn timber beams, as demonstrated by their light weight, high strength, ease of handling, good durability, and economical use of raw materials. In other words, the use of wood composites in I-joists and their I-shape means that the wood content of the joists can be reduced by up to 50% (Tang and Leichti 1984; Zhu *et al.* 2005).

The development of wooden I-joists dates back to the 1920s, when these composite products were tested for use in manufacturing of wooden aircraft spars and ribs. Today, wooden I-joists are present in the construction market with a range of varieties, specifications, and standardization of quality at lower cost and with better performance than traditional wood beams (Nie *et al.* 2013; Wang *et al.* 2019; Chen *et al.* 2021). The most common I-joists in the construction market features wooden flanges and a flat OSB web. Combining of these two components enables each to fulfill a specific function, such as resistance to bending forces in the flanges and shear forces in the web (Zhu *et al.* 2007). The high demand for wooden I-joists in the construction market has made their design and manufacturing process a subject of considerable interest to many researchers. Numerous experimental laboratory studies have been devoted to optimizing and improving the composite's design and development (Abdalla and Sekino 2006; Grandmont *et al*. 2010). Experimental proof has always been considered a necessary practice in order to achieve a satisfactory design and development outcome, especially when the model is simple. However, this experimental approach is limited and sometimes considered inappropriate when the model is complicated. Consequently, highly developed computerized numerical approaches have emerged as a development tool. This numerical approach, or numerical modeling, is based on the finite element method, which enables the model to be approached with great precision and, subsequently, to establish guidelines for efficient design and development. It also saves considerable experimental time and costs (Guan *et al.* 2004; Zhu *et al.* 2005; Grandmont *et al.* 2010).

The first researcher to integrate finite element methods into the study of wood I-joist behavior was Fergus. He was able to analyze the properties of web materials and web openings in the design of the wooden I-joist (Fergus 1979). In 1995, Morris *et al.* determined the shear strength of wooden I-joists with OSB webs, with and without openings, using a two-dimensional finite element method. The OSB panel was considered an orthotropic element with linear elasticity, and Tsai-Hill theory was used as the tensile failure criterion (Morris *et al.* 1995). Bai *et al.* studied the bending behavior of OSB composite beams reinforced with bamboo. Numerical simulations were used to analyze the effects of OSB panels and bamboo with adhesive layers (Bai *et al.* 1999). With the same aim of investigating the properties of OSB panels in wooden I-joists, Grandmont *et al.* studied the sensitivity of a wooden I-joist model to the mechanical properties of OSB panels. They found that the in-plane shear stiffness of OSB panels is the most sensitive parameter in the behavior of wood I-joists (Grandmont *et al.* 2010).

In the past, most studies have focused on the behavior of the flat web of wooden I-joists and on optimizing their mechanical properties by testing various new web materials. Few studies have examined the contribution of other web shapes to the behavior of wooden I-joists. However, other structural shapes, such as corrugated, are widely used in the packaging industry, and in metal and composite structures; they have exhibited excellent performance and behavior (Ma *et al.* 2014). The main advantages of the corrugated form are its light weight and greater resistance to shear stress and shock than a thin, flat form (Ma *et al.* 2014; Pathirana and Qiao 2020). The periodic corrugated form may be considered a novelty in the web of wooden I-joists, but it is not new to steel girders for bridges in civil infrastructure (Wu *et al.* 2020). The webs of corrugated steel I-girders are generally trapezoidal, which improves their behavior and resistance to shear stresses compared to flat, thin webs, which are susceptible to deformation in shear. As a result, the trapezoidal shape avoids the need for a stiffener and reduces the beam's dead weight (Moon *et al.* 2009; Sebastiao and Papangelis 2023).

In previous studies, Zhang *et al.* and Li *et al.* analyzed the impact of corrugated steel web geometry on a steel beam's buckling resistance and identified the most optimal web geometry parameters. They found that the corrugated web could double the I-beam's buckling resistance compared with flat web beams (Li *et al.* 2000; Zhang *et al.* 2000a,b). Several numerical studies have been carried out on corrugated beams. Luo and Edlund studied the buckling behavior of these beams using spline finite element methods. In another study, they also applied a nonlinear finite element method to predict the shear capacity of plate girders with corrugated webs and evaluated the influence of web geometric parameters on the beam's shear capacity (Luo and Edlund 1994, 1996).

The corrugated configuration of the web in the steel beam creates an accordion effect in its behavior, resulting in greater resistance and response to shear forces. When subjected to high shear forces, this type of web can behave according to three different buckling modes: local buckling, global buckling, and interactive shear buckling (Moon *et al.* 2009). Figure 1 illustrates the different buckling behaviors of a corrugated web. The circles shown in the images in Fig. 1 indicate buckling induced in one or more sub-panels of the corrugated web. These corrugated web sub-panels are differentiated by two different colors. The presence of one or a combination of these failure modes depends on the properties and geometric characteristics of the corrugated sheet. Local shear buckling occurs in the form of buckling of individual sub-panels (see the distribution of circles in the first image in Fig. 1). In this buckling mode, each flat rectangular sub-panel of the corrugated sheet is treated alone in the buckling and considered to be supported on all four sides. Global shear buckling is defined by the formation of diagonal buckles across the entire sheet (see the third image in Fig. 1). The entire corrugated sheet is treated as an orthotropic flat panel in this buckling mode. The last buckling mode, interactive buckling, is considered as a combination of local and global buckling (Moon *et al.* 2009; Nie *et al.* 2013; Guo and Sause 2014).

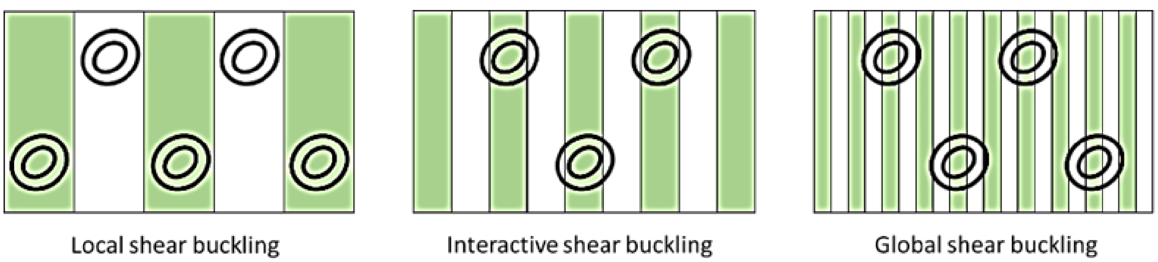


**Fig. 1.** Elastic shear buckling modes of a beam with a corrugated web

In recent years, several in-depth studies have been carried out to investigate and analyze the buckling behavior of the corrugated web of steel beams. Liew *et al.* (2007) and Peng *et al.* (2007) worked on two types of buckling analysis of beams with corrugated web, elastic buckling analysis and a geometrically nonlinear analysis using the Galerkin method. Other researchers, such as Elgaaly *et al.* (1996), Say-Ahmed (2001), Driver *et al.* (2006), Yi *et al*. (2008), Moon *et al.* (2009), and Sause and Braxtan (2001), have devoted their studies to determining analytical solutions for predicting the local and global elastic buckling resistance of the corrugated web of steel beams.

In a recent study, Jiloul *et al.* (2023) investigated the development potential of wooden I-joists with a corrugated web made from wood-based panels. First, these corrugated panels were mechanically characterized to determine their mechanical properties, potential and limitations (Jiloul *et al.* 2023), using bending tests. Joists with corrugated webs were manufactured and tested to assess their mechanical properties. The results obtained were then compared with those of wooden I-joists with OSB web (Jiloul *et al.* 2024).

The present study is a continuation of this earlier work. A numerical approach has been applied to two types of wooden I-joist with different web materials using

Abaqus/CAE software. The first joist is a commercial joist with an OSB web, while the second is an I-joist with a corrugated wood-based panel web. This numerical approach models two types of mechanical tests, a long-span bending test and a short-span bending test. The numerical modeling studied in this article had three main objectives. Firstly, it aimed to establish a numerical model of I-joists with OSB web, and to compare it with the experimental results obtained in the previous study. This first model was considered a reference model for validating the properties of the studied joist components. In the second step, a second numerical model of a wooden I-joist with a corrugated panel web was simulated to determine the unknown shear stiffness of the corrugated panels. This second objective was achieved using the iterative method between the experimental results obtained in the previous study and the numerical modeling results. This method consists of estimating the shear stiffness of corrugated panels input to the model, so that the numerical deformation result matches the experimental result. Finally, this last I-joist model with corrugated panels was also used to study and analyze the buckling behavior of the I-joist corrugated panel web under shear stress.

## MATERIALS AND METHODS

### Experimental Tests

As previously mentioned, a recent study was conducted on the development potential of wooden I-joists with corrugated panel web in which two series of mechanical bending tests were conducted on three types of wooden I-joist. The test series included long- and short-span bending tests to determine the different joist types' bending and shear mechanical properties. The long-span bending test is a bending test with a third-point loading, and the short-span bending test is a test with center-point loading. The proposed test methods are in accordance with ASTM D5055 to evaluate the bending and shear properties of test joists.

Only two of the three joist types tested were examined in this study. The first was a commercial wood I-joist with an OSB web tested in the laboratory. The second type of wood I-joist was an I-joist with a corrugated wood-based panel web, manufactured and tested in the laboratory. Both types of joists tested have the same type and size of wood flange, MSR-2100f-1.8E, 38 mm x 64 mm. However, the web of the joists evaluated differs from commercial joists that have an OSB web of 9.5 mm thickness, whereas the web of the joists manufactured and tested consists of a single type of corrugated panel: Corruven Carrshield 1910Pb (Corruven Inc., New Brunswick, Canada), with a nominal thickness of 19 mm.

The adhesive used to assemble the develop joist specimens was Sikadur®-31 Hi-Mod. Figure 2 shows the configuration of the long-span and short-span bending test of the developed joists. In this structural evaluation of the joists tested, only the 241 mm height was studied, and for the span, two joist spans were selected according to the objective of the bending test. The bending test is performed to failure, and the modes of failure are recorded and analyzed. Additional information on joist components and manufacture, dimensions, bending test procedures and the results obtained in the comparative study are presented and detailed in Jiloul's previous article (Jiloul *et al.* 2024). The different failure modes of the two types of joists are also analyzed in the same article.

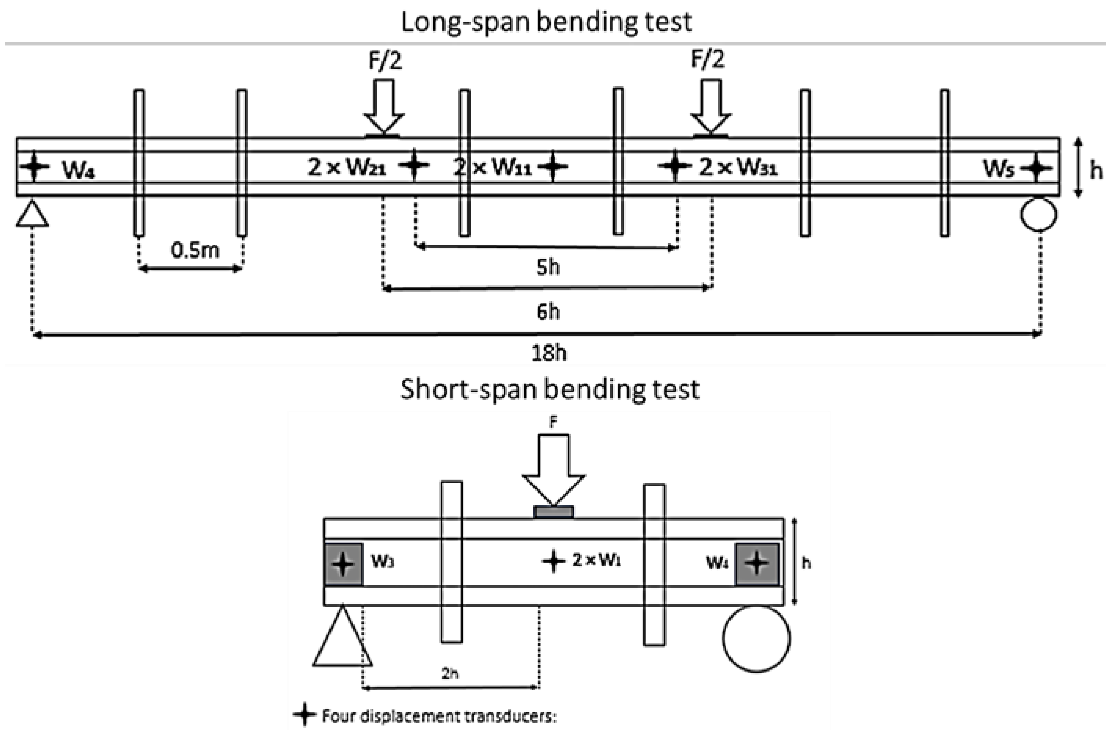


**Fig. 2.** Set-up for long-span and short-span bending tests on developed joists (Jiloul 2024)

## Numerical Simulation

The numerical models for simulating wood I-joists in bending tests were developed using Abaqus/CAE (2021) (Dassault Systèmes Simulia Corp., 2021, Providence, RI, USA). This finite element software has already proved its worth in several previous studies on wood composites and I-joists (Zhu 2003; Blanchet *et al* 2005).

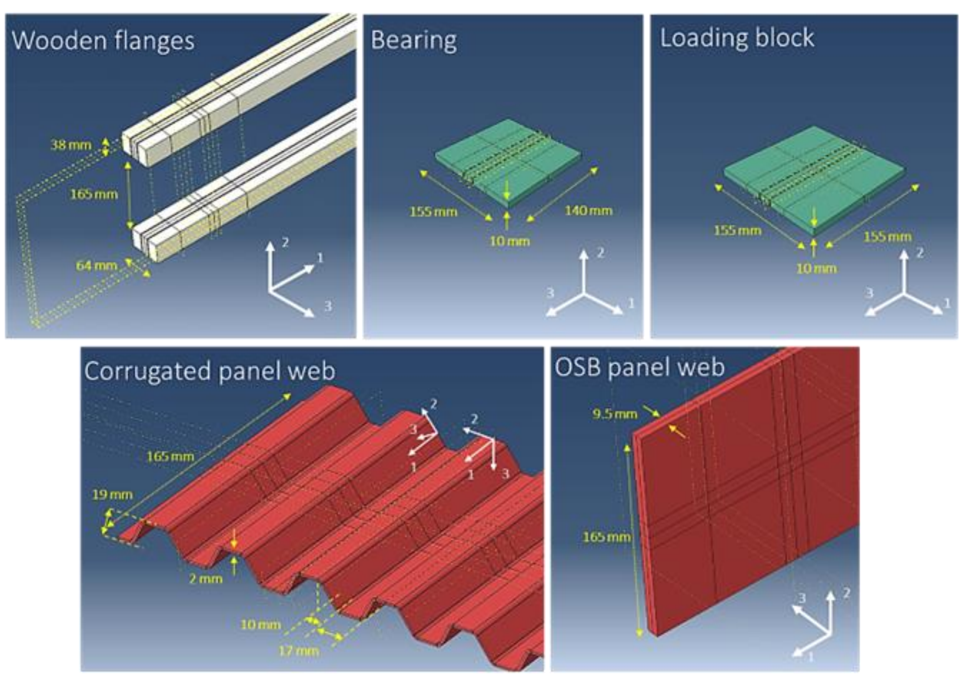


**Fig. 3.** Joist components modeled with their geometric dimensions

*Parts of the model*

Firstly, the flanges of the joist were modeled using an eight-node rectangular solid element C3D8 without the creation or consideration of connection grooves. In contrast, the OSB web was modeled using a four-node straight shell element, S4R. In addition, the load blocks and bearings used in the bending test were also modeled using an eight-node rectangular solid element, C3D8. The size of the representative elements modeled corresponds to the actual dimensions of the various parts of the structure tested. In the case of I-joists with corrugated web, the corrugated panels were modeled by a four-node shell element S4R, which was created by a trapezoidal curve corresponding to the geometric shape of the corrugated panels. Figure 3 shows the various I-joist modeling components tested, together with their geometric dimensions.

*Reference coordinate system for model parts*

Joist components are orthotropic elements, meaning that reference coordinate systems must be applied to each component to match their properties to the reference axes defined for each element. For example, for OSB panels, a global reference system has been chosen whose direction X or 1 corresponds to the panel's strong axis (parallel to fiber direction) and direction Y or 2 corresponds to the panel's weak axis, while direction 3 or Z corresponds to the direction along the panel's thickness. Figure 3 also shows the coordinate system applied on each joist component.

*Mechanical properties of model parts*

All wooden I-joist components, including the flanges and the web of OSB or wood-based corrugated panels, were treated as orthotropic materials, which is considered one of the most important characteristics of wood or wood-based materials. Consequently, for each component, ten mechanical property parameters were defined. These parameters include moduli of elasticity in all three directions ($E_1$, $E_2$, $E_3$), in-plane and through-thickness shear moduli ($G_{12}$, $G_{13}$, $G_{23}$), and Poisson's coefficients ($\nu_{12}$, $\nu_{13}$, $\nu_{23}$), as well as the axial strength of the truss component. The moduli of elasticity considered in this study are the results of compression tests. This hypothesis is justified because the basic Abaqus software used considers only one element behavior. Furthermore, the dominant elastic moduli differ minimally between compression and tension, and their difference creates a variation that does not exceed 1% of the joist bending test result. This has been confirmed by several previous studies (Grandmont *et al.* 2010; Zhu *et al.* 2005a,b, 2007).

For the wooden flanges, MSR-2100f-1.8E mechanically rated lumbers were used. The mechanical properties selected were taken from the mechanical parameters used in simulations carried out in several previous studies (Bodig and Jayne 1993; Grandmont *et al.* 2010). Table 1 shows the elastic properties ($E_1$, $E_2$, $E_3$, $G_{12}$, $G_{13}$, $G_{23}$, $\nu_{12}$, $\nu_{13}$, $\nu_{23}$) and the compressive strength ($R$) of the flanges of the I-joists. The longitudinal direction of the flanges corresponds to property direction 1, while the radial and tangential directions correspond to directions 2 and 3, respectively.

The mechanical properties of OSB panels have also been derived from previous tests (Zhu 2003; Grandmont *et al.* 2010). Table 1 also shows the elastic properties ($E_1$, $E_2$, $E_3$, $G_{12}$, $G_{13}$, $G_{23}$, $\nu_{12}$, $\nu_{13}$, $\nu_{23}$) and the compressive strength ($R$) of the OSB panels used in the modeling. The longitudinal direction of the OSB panels of the I-joists corresponds to property direction 1, while the radial and tangential directions correspond to directions 2 and 3, respectively.

**Table 1.** Technical Properties of the Wood Flanges and OSB Web of I-joists*

| | $E_1$ (MPa) | $E_2$ (MPa) | $E_3$ (MPa) | $G_{12}$ (MPa) | $G_{13}$ (MPa) | $G_{23}$ (MPa) | $\nu_{12}$ | $\nu_{13}$ | $\nu_{23}$ | $R$ (MPa) |
|---|---|---|---|---|---|---|---|---|---|---|
| Wooden flanges | 11528 | 662 | 662 | 666 | 666 | 100 | 0.21 | 0.23 | 0.41 | 37.5 |
| OSB panel | 3650 | 2600 | 130 | 1370 | 240 | 240 | 0.18 | 0.3 | 0.3 | 14.1 |

*(Bodig and Jayne 1993; Zhu 2003; Grandmont *et al.* 2010)
*(E and G are the elasticity and shear moduli respectively)
*(R and nu are compressive strength and Poisson's modulus respectively)
*(Directions 1, 2 and 3 represent longitudinal, radial and tangential directions respectively)

The mechanical properties of the corrugated panels were previously determined in a study carried out on the mechanical characterization of wood-based corrugated panels (Jiloul *et al.* 2023). In this previous study, corrugated panels were characterized by their corrugated shape and their properties were determined by considering them as orthotropic solid flat panels with their nominal thickness. In the Abaqus finite element analysis, the properties required are the properties of corrugated plate panels with their real thickness in a local reference coordinate system that follows the corrugated shape (see Fig. 3).

Initially, elastic strain energy theory determined the modulus of elasticity and the strength of the strong axis of the corrugated panels (axis parallel to the corrugations). This theory was applied by converting these two parameters from a flat orthotropic shape of nominal thickness to a corrugated plate shape of real thickness (Park *et al.* 2016). Equations 1 and 2 show the conversion formula using elastic strain energy:

$$U = \frac{P^2 \times V_{\text{FOS}}}{2 \times E_{\text{FOS}} \times A_{\text{FOS}}} = \frac{P^2 \times V_{\text{CPS}}}{2 \times E_{\text{CPS}} \times A_{\text{CPS}}} \tag{1}$$

$$E_{\text{CPS}} = E_{\text{FOS}} \times \frac{e_{\text{n}}}{e_{\text{r}}} \times \frac{c}{l} \tag{2}$$

In this equation, $E$, $V$, and $A$ represent the modulus of elasticity and the cross-sectional volume of the corresponding panel, either for the flat orthotropic shape (FOS) of nominal thickness ($e_{\text{n}}$), or for a corrugated plate shape (CPS) of real thickness ($e_{\text{r}}$). The symbols (c, l) represent the half-period, half-length of a unit corrugated cell (Park *et al.* 2016). The average values for the modulus of elasticity and strength in the direction of the strong axis were determined based on the results of the corrugated panel characterization study and by applying the theory of elastic energy of strain. Table 2 shows the determined and mechanical properties of corrugated panels.

Concerning the other properties of the corrugated panels, they were initially assumed to be equal to the properties of plywood panels with a thickness of 4 mm and 3 plies. This plywood profile is the minimum size profile available on the market and can be considered as a profile corresponding to corrugated panels with a real thickness of 2 mm with 2 plies (Hughes 2015). Table 2 also shows the estimated mechanical properties of corrugated panels. In this way, Table 2 shows the elastic properties ($E_1$, $E_2$, $E_3$, $G_{12}$, $G_{13}$, $G_{23}$, $\nu_{12}$, $\nu_{13}$, $\nu_{23}$) and the compressive strength ($R$) of the corrugated panel web of the I-joists. The longitudinal direction of the flanges corresponds to property direction 1, while the radial and tangential directions correspond to directions 2 and 3, respectively.

**Table 2.** Determined and Supposed Mechanical Properties of the Corrugated Panel Web*

| | Property (Average Value) | | | | | | |
|---|---|---|---|---|---|---|---|
| | $E_1$ (MPa)$_d$ | $E_2$ (MPa)$_a$ | $E_3$ (MPa)$_a$ | $G_{12}$ (MPa)$_a$ | $G_{13}$ (MPa)$_a$ | $G_{23}$ (MPa)$_a$ | $R$ (MPa)$_d$ |
| Corrugated panel web | 10219.5 | 5000 | 100 | 2000 | 200 | 200 | 29.33 |

d = Experimentally determined a = Assumed value

*(Hughes 2015; Jiloul *et al.* 2023)
*(E and G are the elasticity and shear moduli respectively)
*(R and nu are compressive strength and Poisson's modulus respectively)
*(Directions 1, 2 and 3 represent longitudinal, radial and tangential directions respectively)

A sensitivity study was carried out to better understand the effect of these corrugated panel properties and the proposed hypothesis. In this sensitivity study, the various assumed initial properties ($E_2$, $E_3$, $\nu_{12}$, $\nu_{13}$, $\nu_{23}$, $G_{12}$, $G_{13}$, $G_{23}$) of the corrugated panel were modified to analyze their effect on the behavior of the joist during bending tests and to determine the dominant elastic property of the corrugated panel web. Then, the iterative method defined above is used between experimental and numerical results to estimate the value of this dominant web parameter.

Finally, the loading blocks and bearings were modeled as isotropic steel materials as used in the joist bending test.

## Step

The type of behavior chosen for the different models was a general non-linear static behavior with sufficient increments to carry out the modeling analysis. This choice of behavior makes it possible to determine the out-of-plane deformation of different model components during loading.

## Interaction Modeling

Three types of interaction were selected in the modeling of wooden I-joists. Figure 4 shows these different types of interaction.

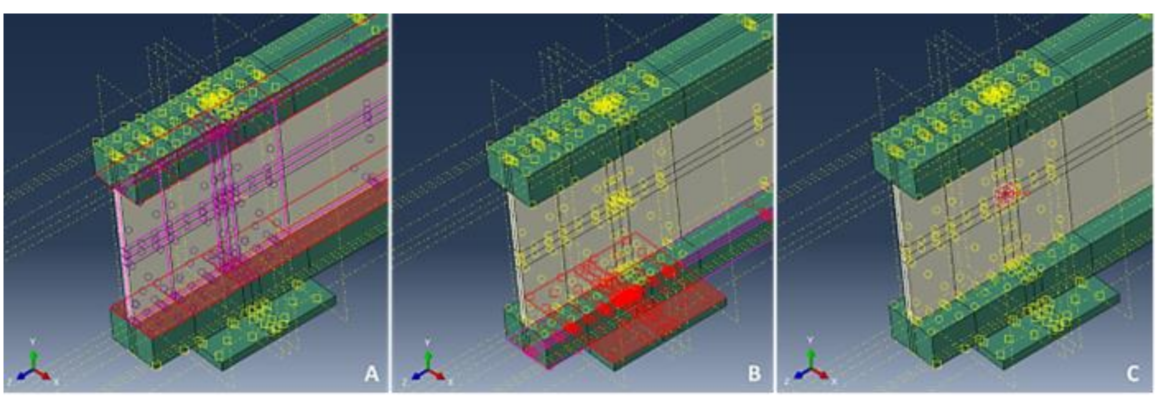


**Fig. 4.** Interactions selected for modeling the I-joist: (A) Interaction between flanges and web, (B) Interaction between flanges and bearings and loading blocks, and (C) Deformation measurement interaction

In bending tests on wooden I-joists with OSB or corrugated panel webs, all specimens failed first either at the flange or the web. Failure of the flange-web joint was rare, and in those cases when it did occur, it was considered a deformation sequence following flange and web failure. As a result, the adhesives used to join the flanges and web were considered to be very rigid in relation to the properties of the joist elements tested, and the connection between the flanges and web was therefore considered to be a rigid "Tie"-type connection, as shown in Fig. 4A. This type of connection links two separate surfaces in such a way that there is no relative movement between them and corresponds to the joists tested.

For contact between joist flanges and metal parts, whether with bearings or load blocks, two types of behavior have been selected. Normal behavior, represented by hard contact, and tangential behavior, represented by penalty friction, with a coefficient of friction of 0.6 considered between steel and wood (see Fig. 4B).

The interaction assumptions used in this study have also been applied in simulations of previous studies, for bending tests on wooden I-joists (Grandmont *et al.* 2010; Rouaz and Bouzid 2023).

In the joist bending tests, a strain-capture system was installed at eight points along the length of the joist under test (see Fig. 1) to record the deformation of the specimens on its neutral axis (Jiloul *et al.* 2024). For the simulation, coupling stresses were applied in the same area of the joists to determine their deformations, which is illustrated in Fig. 4C. As a reminder, coupling stresses allow the motion of a surface to be constrained to the motion of a single point without influencing the overall behavior of the structure.

## Loading and Boundary Conditions

In the bending test, the hydraulic cylinder is used to apply a load to the joist specimens at a certain speed. In the numerical simulation, the applied loads are replaced by equivalent linear displacements also applied to the loading block. From this applied displacement, the Abaqus software generates the corresponding loads. Linear displacements are estimated based on experimental behavior curves depending on joist types and bending tests. For long-span bending tests, a displacement of 65 mm is applied to the joists tested. Displacements of 25 mm are applied to joist specimens tested in short-span bending tests. Figure 5 shows the linear displacement applied and the bearing selected for the bending test.

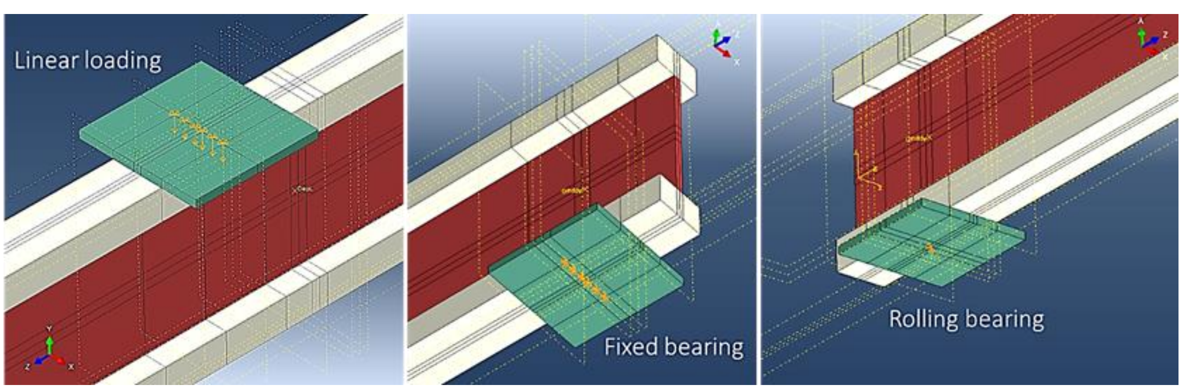


**Fig. 5.** Linear displacement and bearing selected for the bending test

Regarding boundary conditions, the tested joists are placed on two different supports, the first being a fixed support to limit joist displacements in all three directions ($u_1 = 0$, $u_2 = 0$, $u_3 = 0$). This bearing is modeled as a linear bearing to enable the bearing elements to follow the rotational deformation of the joist under test, which corresponds to the deformation of the joist during the bending test. The second bearing is a rolling bearing, which retains only vertical and horizontal displacements perpendicular to the length of the joist ($u_1 = 0$, $u_2 = 0$). This support is simulated as a point of bearing to release the permitted rotation and displacement of the joist under test.

Other bearings were also added to the joist model tested. Punctual bearings were applied along the joist flanges every 600 mm. These bearings represent lateral supports designed to prevent joist spillage during loading.

## Mesh Size

A convergence analysis was performed to determine the mesh size required and appropriate for the joists tested. The mesh size is chosen to guarantee sufficiently precise results and a reasonable calculation time. The mesh is applied using a brick element distributed over the entire sample. This element adapts to the joist geometry and ensures continuous meshing between all joist components. The mesh size considered is 0.009, which means that for every 64 mm, there are 7 brick elements. A finer mesh was generated in the connection zone between the footings and the web to ensure continuous meshing between these two elements. Figure 6 shows the mesh applied to simulations of the two joist types tested.

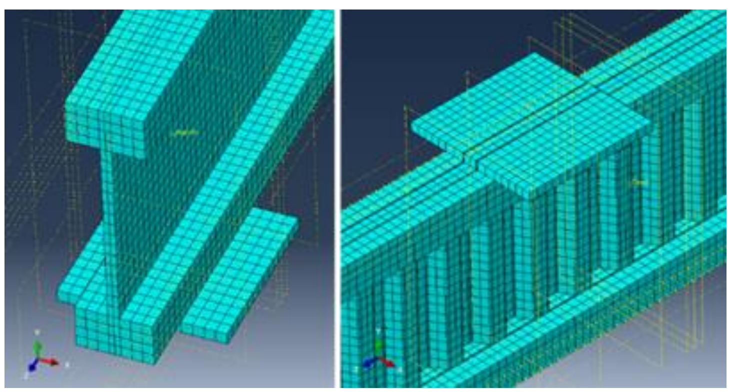

**Fig. 6.** The mesh selected for modeling the tested joist

## Calculation of the Mechanical Properties of Joists Tested in a Bending Test

In numerical modeling, the specific displacement is applied progressively to the load blocks of the joist under test. This displacement is devised over several increments. The size and speed of the increments depend on the complexity of the model and its mesh and on the properties of the modeled structure. The software generates the associated applied forces for each specified displacement increment. The software also calculates the deformations and stresses generated in the modeled structure and in the various directions for each specified displacement increment.

Based on the behavior curves of different types of model joists, the mechanical properties of model joists in long-span and short-span bending tests are determined. The joist properties for the long-span bending test include the maximum efforts supported by the joist: the maximum force ($F_{max}$), the bending moment ($M$), the supported shear force

($V$), and the joist's local ($EI_s$) and global ($EL_g$) stiffness, as well as the shear deformation coefficient ($K_s$). While the mechanical properties determined by the short-span bending test are the maximum force ($F_{max}$), the shear force supported ($V$), and the global joist stiffness ($EI_c$). The calculation formulas for these properties are detailed in the previous study carried out on the structural evaluation of I-joists with corrugated panel web (Jiloul *et al.* 2024).

## RESULTS AND DISCUSSION

### Modeling I-joists with OSB web in long-span bending

Using Abaqus software, the behavior curve of an I-joist with an OSB web and the joist's mechanical properties in long-span bending tests were determined. Figure 6 shows the experimental behavior curves of the wooden I-joist with OSB web for the seven specimens tested in the previous study and the behavior curve obtained numerically. Table 3 compares the experimental and numerical mechanical properties of I-joists. The experimental mechanical properties mentioned in the table were also taken from Jiloul's previous study (Jiloul *et al.* 2024). The elastic properties $EI_g$, $EI_s$, and $K_s$ were derived from the experimentally or numerically measured displacements and calculated using the same methods as in the previous study (Jiloul *et al.* 2024).

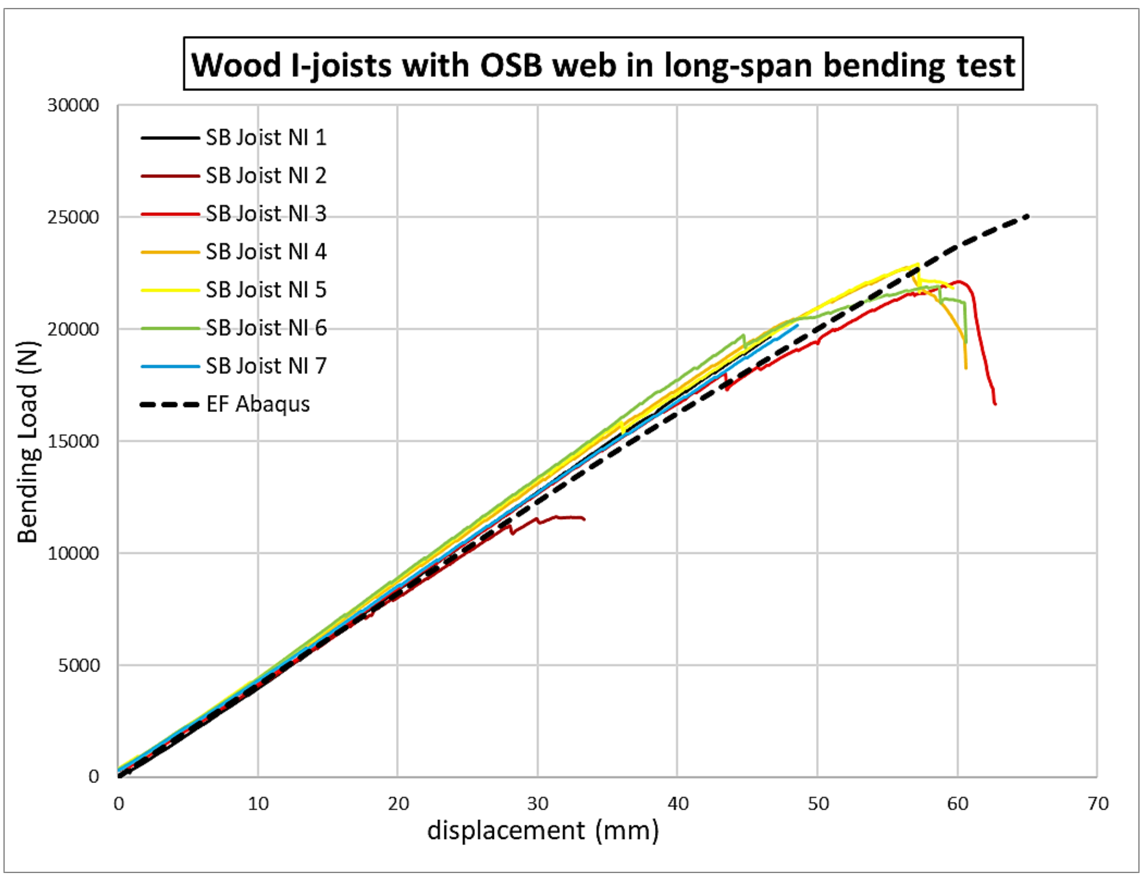


**Fig. 7.** Experimental and numerical behavior curves of the wooden I-joist with OSB web in long-span bending tests (Jiloul, 2024)

**Table 3.** Comparison of Experimental and Numerical Mechanical Properties of I-Joists with OSB Web in Long-Span Bending Tests (Jiloul *et al.* 2024)

| | Experimental Results | | Numerical Results | |
|---|---|---|---|---|
| | Average V | (σ; COV) | Value | Difference |
| $F_{max}$ (kN) | 20.17 | (3.96 ; 20%) | 25.04 | -24% |
| $V$ (kN) | 10.09 | (1.99 ; 20%) | 12.52 | -24% |
| $M$ (kN.m) | 14.6 | (2.86 ; 20%) | 18.13 | -24% |
| $EI_g$ ($10^6$ kN.mm²) | 584.74 | (19.95 ; 4%) | 543.37 | 7% |
| $EI_s$ ($10^6$ kN.mm²) | 681.7 | (44.64 ; 12%) | 625.86 | 8% |
| $K_s$ (kN) | 1894.07 | (62.33 ; 3%) | 1761.58 | 7% |

A look at Fig. 7 clearly shows a good correlation between experimental and numerical behavior curves, especially regarding the elastic behavior of the joist. Firstly, for elastic joist properties, such as global and local stiffness and shear strain coefficient, the difference between experimental and numerical results did not exceed 8%, regardless of the web properties, as shown in Table 3. This difference remains acceptable, given the coefficients of variation of the seven joists tested and the natural variability of wood's mechanical properties (Bodig and Jayne 1993).

As far as internal forces are concerned, there was a non-negligible difference between experimental and numerical results. The difference between the internal efforts is 24% primarily because the numerical model is an idealized model in which singularities and wood defects, such as knots, splits, and cracks, are not modeled or considered in the modeling.

In addition, the butt joints of the footings or web are also not modeled. However, in long-span bending tests on wooden I-joists with OSB web, it was found that failures occurred mainly in the upper or lower flanges due to the presence of knots or butt joints (Jiloul *et al.* 2024). Consequently, the large difference in internal efforts between the experimental and numerical results can be explained by the singularities, defects, and joints present in the experimental model and not considered in the numerical model.

Using Abaqus software, the deflection and compressive stress distribution in the modeled joist were determined. Figure 8 shows the distributions of these two parameters over half the span of a wooden I-joist tested in long-span bending. The greatest stress is exerted on the lower and upper flanges of the joist. This corresponds to the aim of the long-span bending test, in which the properties of the joist flanges are primarily evaluated. In this test, the upper flange is subjected to compressive stress and the lower flange to tensile stress. For this reason, the first failures in this test occurred either in the upper flanges due to stress concentration in singularities or defects in the timber used, or in the lower flanges due to the presence of butt joints. The distribution of shear stress and deflection in the wooden I-joist with OSB web obtained in this simulation was similar to that obtained in the simulation carried out by the Grandmont study (Grandmont *et al.* 2010).

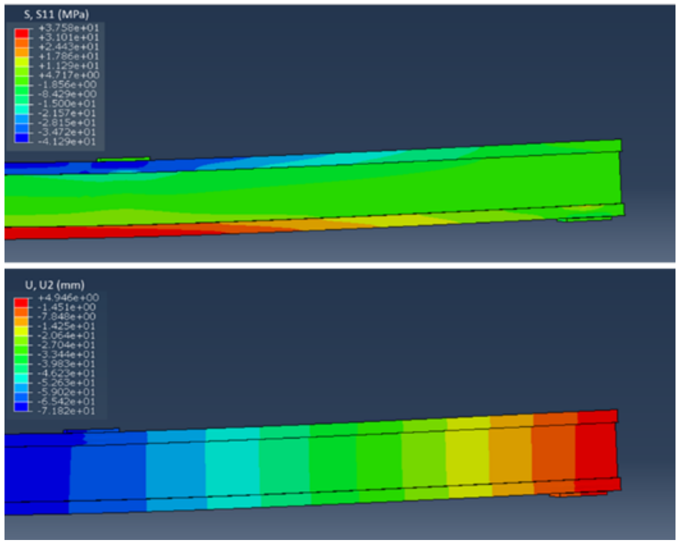


**Fig. 8.** Behavior of wooden I-joist with OSB web tested in long-span bending: (a) stress distributions, and (b) strain distributions over half-span

## Modeling I-joists with OSB Web in Short-Span Bending

As with the long-span bending test, the behavior curves and mechanical properties of I-joists with OSB web in short-span bending were determined using Abaqus software (Dassault Systèmes Simulia Corp., 2021, Providence, RI, USA). Figure 9 shows the load-displacement curves resulting from the simulation. It also shows the behavior curves of seven joists experimentally tested in the same bending test. Table 4 compares the mechanical properties obtained numerically and experimentally.

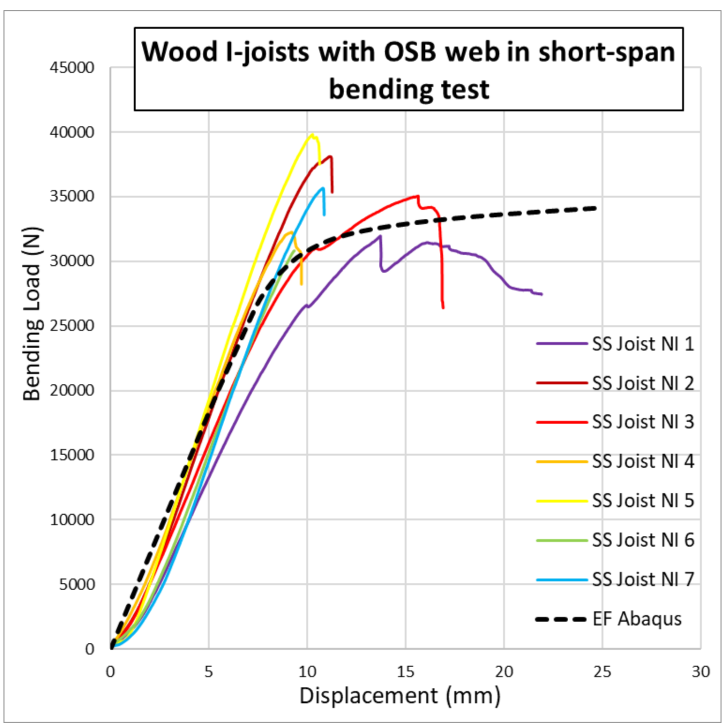


**Fig. 9.** Experimental and numerical behavior curves of wooden I-joist with OSB web in short-span bending tests (Jiloul 2024)

**Table 4.** Comparison of Experimental and Numerical Mechanical Properties of I-joists with OSB Web Short-span Bending Tests (Jiloul *et al.* 2024)

| | Experimental Results | | Numerical Results | |
|---|---|---|---|---|
| | Average Value | (σ; COV) | Value | Difference |
| $F_{max}$ (kN) | 34.81 | (3.10 ; 9%) | 34.13 | 2% |
| $V$ (kN) | 17.4 | (1.55 ; 9%) | 17.07 | 2% |
| $EI_c$ ($10^6$ kN.mm²) | 175.86 | (18.54 ;11%) | 185.28 | -5% |

Good alignment was observed between numerical and experimental results in the elastic part of the joist behavior curves. Table 4 also shows that the difference between the overall joist stiffnesses determined did not exceed 5%, which is acceptable and expected, especially as the coefficient of variation between the seven joists tested exceed this value. Regarding the maximum supported effort, the maximum force estimated by the numerical simulation was close to that obtained experimentally. These small differences can be explained by the fact that in this test, the maximum stress is supported by the web and not by the flanges, unlike in the long-span test. In addition, the singularities and defects of the OSB are less present in the test with a much shorter span than in the long-span test. Consequently, the numerical model provides an improved representation of the joist model tested.

The two numerical joist simulations carried out above show a good correlation with the experimental results, with the differences remaining acceptable. Therefore, they make it possible to validate the mechanical properties assumed at the start of the study, both those of the wooden flanges and those of the OSB web. Consequently, these two models are considered reference models for the following modeling work. Verification of the flange properties was necessary for the numerical simulation study of the second I-joist model with corrugated web. In this study, the same type of wooden flange was used, but the focus was on the unknown properties of the corrugated web.

## Modeling I-joist with Corrugated Panel Web in a Long-span Bending Test

The properties required of the corrugated panel web for numerical simulation are moduli of elasticity in all three directions, shear moduli in plane and thickness, the Poisson coefficients, and strength in the panel's strong axis. Of these ten parameters, only the modulus of elasticity in the strong axis direction is known (see methods section), and the others have not yet been determined.

For this reason, the properties of plywood panels with a minimum thickness were chosen as the initial parameter for corrugated panels, given that the thickness and composition of corrugated panels are similar to plywood panels. Next, a sensitivity study was conducted to determine the effect of each parameter on joist behavior in long-span bending tests. This sensitivity study consisted of varying each parameter while fixing the others and seeing their influence on the results of the mechanical properties of the joists tested.

Tables 5 and 6 present a sensitivity study of parameters $E_2$ and $E_3$. Varying the modulus of elasticity $E_2$ of the weak axis of the corrugated panels was found to have a negligible effect on the calculations of the global and local stiffnesses and the shear deformation coefficient of the simulated joist. The variation of this stiffness from 10000 MPa to 100 MPa, which represents the possible range of variation of this parameter, resulted in a variation of no more than 0.8% of the mechanical joist properties listed in Table 5. The effect of varying $E_2$ on maximum force is discussed in another section of this article. The variation in $E_3$ modulus of elasticity had no effect on the calculation of mechanical joist properties, as shown in Table 6. The sensitivity study was also carried out on Poisson coefficients, and the results obtained showed that they also had a minimal effect on joist properties, not exceeding 0.001%.

Tables 7, 8, and 9 show the variation in-thickness shear moduli of the corrugated panels on the mechanical properties of the simulated joists. The influence of the variation in $G_{13}$ and $G_{23}$ accounted for no more than 0.08% of the variation in joist properties. Consequently, these two parameters are not considered to be the dominant ones with a considerable influence on the calculation of local and global stiffness and shear deformation coefficient. In contrast, Table 9 clearly shows that variation in the $G_{12}$ modulus of elasticity had a considerable influence on the calculation of joist properties. Consequently, the $G_{12}$ in-plane shear modulus of corrugated panels is considered the most critical corrugated panel web parameter in the bending behavior of the long-span I-joist.

**Table 5.** Variation of Long-span Bending Joist Properties as a Function of Modulus of Elasticity $E_2$

| $E_2$ (MPa) | $F_{max}$ (kN) | | $EI_g$ ($10^6$ kN.mm²) | | $EI_s$ ($10^6$ kN.mm²) | | $K_s$ ($10^6$ kN.mm²) | |
|---|---|---|---|---|---|---|---|---|
| | Value | Difference | Value | Difference | Value | Difference | Value | Difference |
| 10000 | 13.47 | | 427.82 | | 591.55 | | 1367.46 | |
| 5000 | 13.44 | 0.19% | 427.07 | 0.18% | 591.19 | 0.06% | 1364.95 | 0.18% |
| 1000 | 12.75 | 5.34% | 425.25 | 0.60% | 590.31 | 0.21% | 1358.90 | 0.63% |
| 500 | 12.49 | 7.28% | 424.47 | 0.78% | 589.93 | 0.27% | 1356.29 | 0.82% |

**Table 6.** Variation of Long-span Bending Joist Properties as a Function of Modulus of Elasticity $E_3$

| $E_3$ (MPa) | $F_{max}$ (kN) | | $EI_g$ ($10^6$ kN.mm²) | | $EI_s$ ($10^6$ kN.mm²) | | $K_s$ ($10^6$ kN.mm²) | |
|---|---|---|---|---|---|---|---|---|
| | Value | Difference | Value | Difference | Value | Difference | Value | Difference |
| 1000 | 13.44 | | 427.07 | | 591.19 | | 1364.95 | |
| 500 | 13.44 | 0.00% | 427.07 | 0.00% | 591.19 | 0.00% | 1364.95 | 0.00% |
| 100 | 13.44 | 0.00% | 427.07 | 0.00% | 591.19 | 0.00% | 1364.95 | 0.00% |

**Table 7.** Variation of Long-span Bending Joist Properties as a Function of Shear Modulus $G_{13}$

| $G_{13}$ (MPa) | $F_{max}$ (kN) | | $EI_g$ ($10^6$ kN.mm²) | | $EI_s$ ($10^6$ kN.mm²) | | $K_s$ ($10^6$ kN.mm²) | |
|---|---|---|---|---|---|---|---|---|
| | Value | Difference | Value | Difference | Value | Difference | Value | Difference |
| 2000 | 13.44 | | 427.07 | | 591.19 | | 1364.95 | |
| 1500 | 13.44 | 0.07% | 427.03 | 0.01% | 591.17 | 0.00% | 1364.84 | 0.01% |
| 1000 | 13.43 | 0.14% | 426.99 | 0.02% | 591.15 | 0.01% | 1364.70 | 0.02% |
| 500 | 13.41 | 0.23% | 426.92 | 0.03% | 591.12 | 0.01% | 1364.47 | 0.04% |
| 100 | 13.39 | 0.37% | 426.74 | 0.08% | 591.03 | 0.03% | 1363.88 | 0.08% |

**Table 8.** Variation of Long-span Bending Joist Properties as a Function of Shear Modulus $G_{23}$

| $G_{23}$ (MPa) | $F_{max}$ (kN) | | $EI_g$ ($10^6$ kN.mm²) | | $EI_s$ ($10^6$ kN.mm²) | | $K_s$ ($10^6$ kN.mm²) | |
|---|---|---|---|---|---|---|---|---|
| | Value | Difference | Value | Difference | Value | Difference | Value | Difference |
| 2000 | 13.44 | | 427.07 | | 591.19 | | 1364.95 | |
| 1500 | 13.44 | 0.07% | 427.01 | 0.01% | 591.17 | 0.00% | 1364.78 | 0.01% |
| 1000 | 13.42 | 0.15% | 426.94 | 0.03% | 591.14 | 0.01% | 1364.54 | 0.03% |
| 500 | 13.41 | 0.24% | 426.82 | 0.06% | 591.09 | 0.02% | 1364.13 | 0.06% |
| 100 | 13.39 | 0.42% | 426.82 | 0.06% | 590.97 | 0.04% | 1364.14 | 0.06% |

**Table 9.** Variation of Long-span Bending Joist Properties as a Function of Shear Modulus $G_{12}$

| $G_{12}$ (MPa) | $F_{max}$ (kN) | | $EI_g$ ($10^6$ kN.mm²) | | $EI_s$ ($10^6$ kN.mm²) | | $K_s$ ($10^6$ kN.mm²) | |
|---|---|---|---|---|---|---|---|---|
| | Value | Difference | Value | Difference | Value | Difference | Value | Difference |
| 2000 | 13.44 | | 427.07 | | 591.19 | | 1364.95 | |
| 1500 | 13.41 | 0.23% | 392.48 | 8.10% | 574.50 | 2.82% | 1249.67 | 8.45% |
| 1000 | 13.31 | 0.97% | 338.22 | 20.80% | 534.24 | 9.63% | 1071.72 | 21.48% |
| 500 | 11.61 | 13.65% | 239.85 | 43.84% | 406.22 | 31.29% | 756.90 | 44.55% |
| 100 | 3.91 | 70.88% | 78.28 | 81.67% | 103.54 | 82.49% | 251.01 | 81.61% |

This sensitivity study is not the first of its kind. In a previous study, Fergus found that the modulus of elasticity of flanges along the longitudinal axis was the parameter with the most influence on the results of long-span bending tests on wooden I-joists (Fergus 1979). More recently, in another study on the same subject, Grandmont *et al.* (2010) confirmed that the modulus of elasticity in the strong axis of the flanges and the shear modulus in the plane of the web are the only parameters that need to be determined experimentally to carry out a correct simulation corresponding to the experimental test. It was also found that variations in $E_2$ and $E_3$, $\nu_{12}$, $\nu_{13}$, $\nu_{23}$, $G_{13}$, and $G_{23}$ had virtually no considerable effect on the calculation of the overall deflection of wooden I-joists in long-span deflection tests (Grandmont *et al.* 2010). The results of these studies agree with the results obtained in the present study, even though the web studied was corrugated and the comparative studies were carried out on a flat OSB web.

In the authors' previous (Jiloul *et al.* 2023) mechanical characterization of corrugated wood-based panels, the in-plane shear modulus was difficult to determine due to the particular shape of the panels. The determination of these shear properties became the subject of the present study. Having conducted long-span bending tests on wooden I-joists with corrugated panel webs in the previous study, numerical simulation of this test was carried out to estimate the corrugated panel's in-plan shear moduli.

With the use of the iterative method between experimental and numerical results, the shear modulus of the corrugated panels was estimated. This modulus also corresponds to the most negligible possible differences between the mechanical properties of simulated and tested joists. Figure 10 shows the behavior curves of seven experimentally tested I-joists, and the behavior curves of modeled I-joists as a function of shear modulus in the $G_{12}$ plane of the corrugated panel web. Table 10 compares the mechanical properties experimentally and numerically obtained as a function of the in-plane shear modulus of I-joists in long-span bending tests.

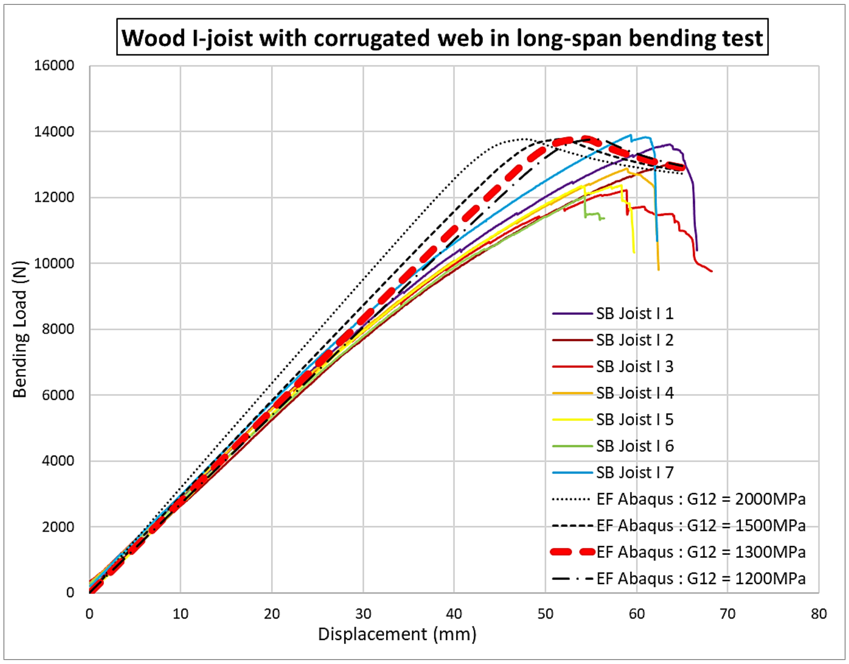


**Fig. 10.** Experimental and numerical behavior curves of a wooden I-joist with a corrugated panel web in long-span bending tests (Jiloul 2024)

**Table 10.** Comparison of Experimental and Numerical Mechanical Properties of I-joists with Corrugated Panel Web in Long-span Bending Tests (Jiloul *et al.* 2024)

| | | $F_{max}$ (kN) | | EIg (10^6 kN.mm²) | | EIs (10^6 kN.mm²) | | $K_s$ (10^6 kN.mm²) | |
|---|---|---|---|---|---|---|---|---|---|
| | | Value | Difference | Value | Difference | Value | Difference | Value | Difference |
| Experimental Results | | 12.86 | | 377.58 | | 605.19 | | 1196.73 | |
| Numerical Results | $G_{12}$ (MPa) = 2000 | 13.79 | -7.20% | 423.70 | -12.21% | 589.64 | 2.57% | 1353.70 | -13.12% |
| | $G_{12}$ (MPa) = 1500 | 13.78 | -7.16% | 389.54 | -3.17% | 572.61 | 5.38% | 1239.97 | -3.61% |
| | **$G_{12}$ (MPa) = 1300** | **13.78** | **-7.18%** | **371.22** | **1.69%** | **560.80** | **7.34%** | **1179.53** | **1.44%** |
| | $G_{12}$ (MPa) = 1200 | 13.79 | -7.19% | 360.64 | 4.49% | 553.03 | 8.62% | 1144.84 | 4.34% |

In conclusion, the in-plane shear modulus of corrugated panels that best matched the numerical simulation to obtain results close to those obtained experimentally was 1300 MPa. This value was chosen to match the overall stiffness and, above all, the shear deformation coefficients between the experimental and numerical results, because the two last parameters reflect the contribution of the corrugated panel web to the behavior of the joist in long-span bending tests. As a reminder, this elastic shear property corresponds to the property of a corrugated panel with its actual thickness in a local reference coordinate system that follows the corrugated shape.

## I-joist with a Corrugated Panel Web in a Short-span Bending Test

The mechanical properties of corrugated panels identified by modeling an I-joist with a corrugated web in a long-span bending test were taken as reference properties. These properties are introduced in the case of a model of the same type of joist but in short-span bending tests. Figure 11 shows the behavior of seven I-joists with a corrugated panel web in short-span bending tests. It also shows the behavior curves of the numerical models, taking into account the web properties identified by modeling. Table 11 compares the joist's mechanical properties in short-span bending tests obtained experimentally and by numerical simulation.

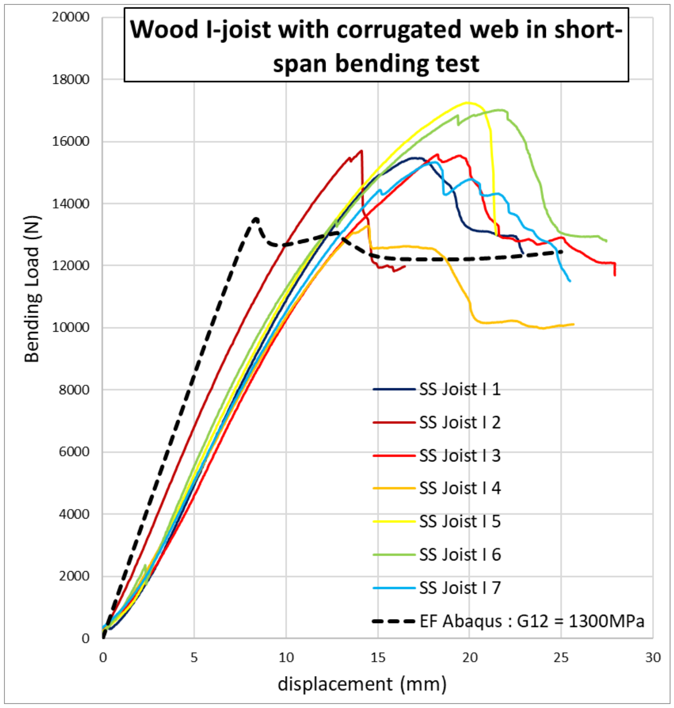


**Fig. 11.** Experimental and numerical behavior curves of a wooden I-joist with a corrugated panel web in sort-span bending tests (Jiloul 2024)

**Table 11.** Comparison of Experimental and Numerical Mechanical Properties of I-joists with Corrugated Panel Web in Sort-span Bending Tests (Jiloul, 2024)

| | Experimental Results | | Numerical Results | |
|---|---|---|---|---|
| | Average Value | (σ; COV) | Value | Difference |
| $F_{max}$ (kN) | 15.66 | (1.20; 8%) | 13.51 | 14% |
| $EI_c$ ($10^6$ kN.mm²) | 44.46 | (3.89; 9%) | 57.01 | -28% |

The behavioral curve and mechanical properties obtained numerically show some difference from the experimental test results. This difference reaches 14% for maximum force and 28% for overall stiffness. This difference could be due to several factors. First, the variability of the mechanical properties of wood-based joist components is one factor. For example, when characterizing corrugated panels, there is an inevitable coefficient of variation in the mechanical properties of corrugated panels in compression or tension. This coefficient of variation can be as high as 23% in some cases. Consequently, some variability is also possible in the numerically determined shear moduli of corrugated panels, and this variability can improve the cohesion between numerical and experimental results of corrugated web joists in short-span bending tests. In addition, joists with corrugated web are manually manufactured, with a certain margin of error. This margin of error can be either height precision or horizontality along the entire length of the manufactured joist (Jiloul *et al.* 2023). Consequently, these two factors may be responsible for the discrepancy between experimental and numerical results.

In the present study, the shear modulus of corrugated panels was chosen based on the iterative method between experimental and numerical results of joists tested in long-span bending tests and not in short-span tests. This was because the shear deformation coefficient is determined by the results of long-span joist tests. This deformation coefficient represents the contribution of the web alone to the overall deformation of the joist and is therefore considered a reliable parameter that concerns only the corrugated web in the iterative method. In the case of short-span bending tests, the overall stiffness determined includes the contribution of the web and flanges. Although, the contribution of the flanges is negligible, given the span of the joist tested. Whereas this bending test is primarily designed to determine the shear strength of the joist supported by its web.

## Behavior of Corrugated Panels in I-joists in Long-span Bending Tests

In long-span bending tests on I-joists with a corrugated web, failures were generally observed in the corrugated panels with a particular behavior. The appearance of the failure of the web during the long-span bending test, when it was supposed to appear in the flanges, defeats the test's purpose, which is primarily to assess the performance of the flanges and not the web. This means that the corrugated web is not strong enough to resist failure up to the point of failure of the flanges. It was therefore necessary to analyze the behavior of this corrugated web to understand it. Using numerical modeling described in "Modeling I-joist with Corrugated Panel Web in a Long-span Bending Test", the behavior of I-joist with corrugated web was reproduced and compared with experimental results and observations. Figure 12 shows the evolution of behavior curves during long-span bending tests, obtained both experimentally and numerically. This evolution is accompanied by Fig. 13, which shows the stages in the evolution of web behavior, using synchronization between mechanical test results and numerical simulations. This includes stress distribution and displacements in the $U_1$ and $U_3$ directions.

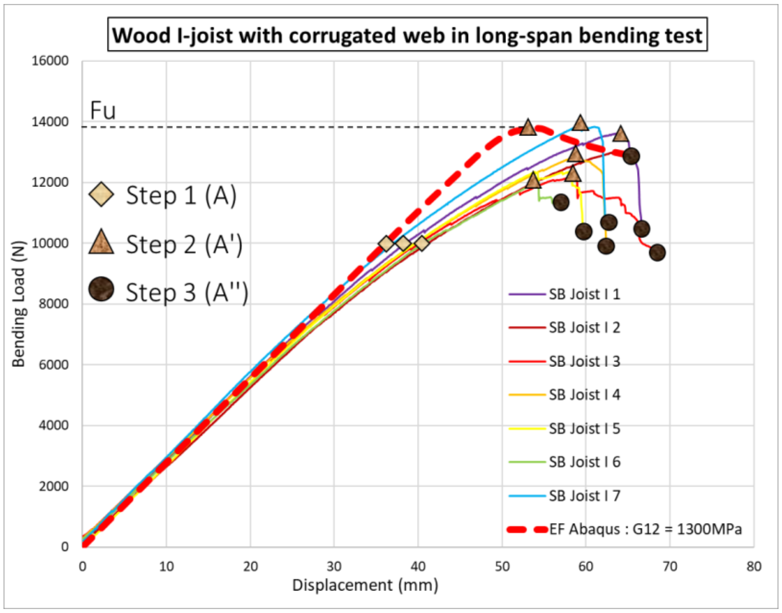


**Fig. 12.** The evolution of behavior curves for I-joists with corrugated web during long-span bending tests, obtained both experimentally and numerically (Jiloul 2024)

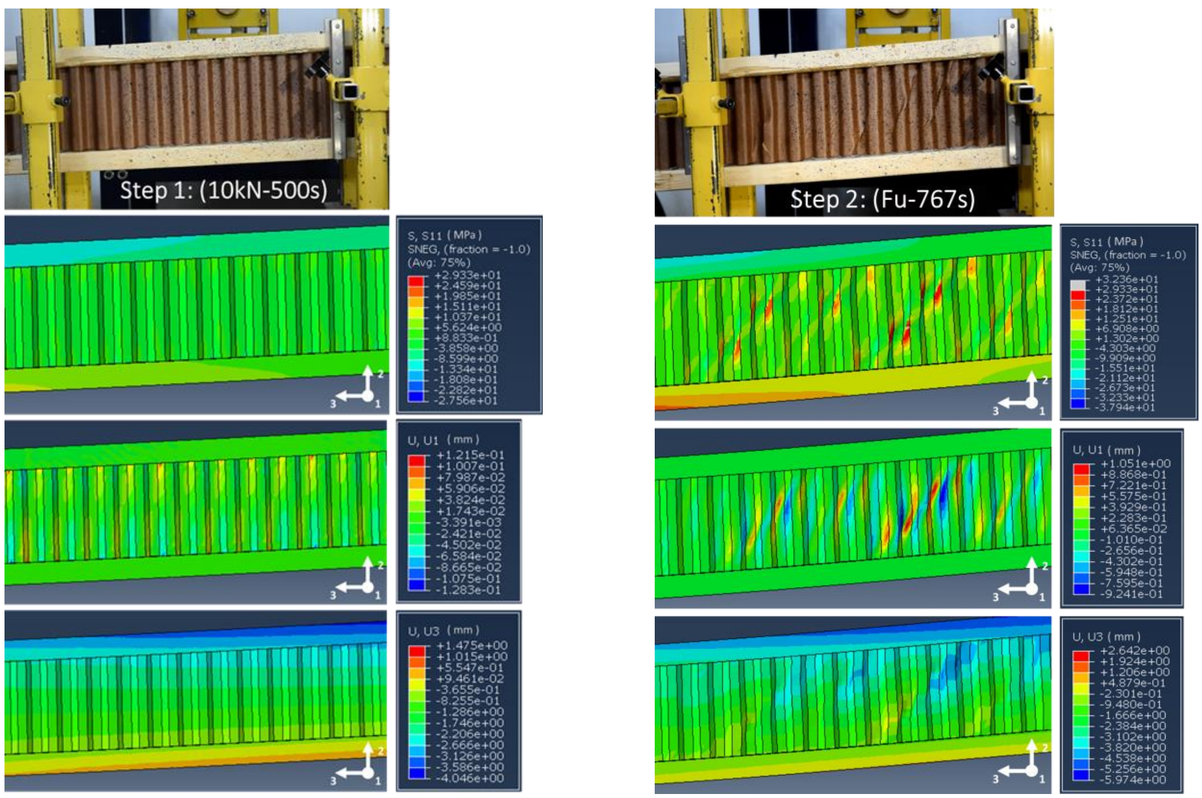

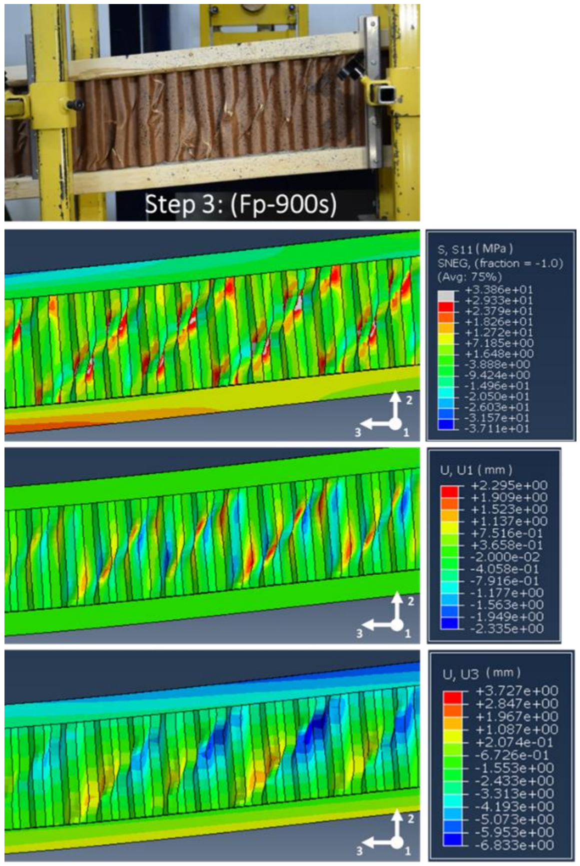


**Fig. 13.** Stages in the evolution of web behavior, using synchronization between mechanical test results and numerical simulations (Steps 1, 2, and 3) (Jiloul 2024)

The behavior of the corrugated web was analyzed in three main stages, chosen according to the evolution of the web failure:

1- Figure 13: Step 1 illustrates point A of the joist behavior curve in Fig. 12, corresponding to a 10 kN load. From the initial load to this point, no out-of-plane deformation visibly has occurred in the corrugated web or in the complete structure. This means that the joist still exhibits linear elastic behavior. This is also confirmed by examining the distribution of stresses and strains ($U_1$ and $U_3$) at this point on the curve. These parameters are uniformly distributed throughout the corrugated web of the joist.

2- On reaching point A' on the behavior curve, which corresponds to the joist force $F_u$, different stress and deformation distributions begin to appear in the joist web. Figure 13: Step 2 shows the appearance of a non-uniform stress distribution and stress concentrations that localize in a sub-panel and sometimes propagate from the center of a sub-panel to adjacent sub-panels. From the view of the deformation of the web sub-panels in different directions, Fig. 13 Step 2 clearly shows that out-of-plane deformations are introduced in the X ($U_1$) and Z ($U_3$) directions. Furthermore, these deformations also take the form of stress distributions, so they localize within the sub-panels and/or continue to propagate beyond the width of the sub-panels and affect adjacent sub-panels. At this stage of the joist's behavior, the joist web is heading towards interactive buckling.

The corrugated panels used to consist of two layers of wood veneer with cellulose sheets as the outer layer (Jiloul *et al.* 2023). This outer layer is not considered in the numerical simulations, as its contribution is negligible. In contrast to the numerical simulations, this layer does not allow out-of-plane deformation to be clearly seen in the photo during mechanical testing, as clearly indicated in the numerical simulations.

3- Step 3 of corrugated web behavior in Fig. 13 begins at point A and extends to point A" on the behavior curve in Fig. 12. This stage represents the plastic part of the web behavior, so the failure modes noted above develop up to the final failure of the joist. First, the continuity of loading after the ultimate joist force enabled a precise analysis of the development of interactive buckling in the corrugated web. This interactive buckling developed in three sub-panels of the corrugated web, comprising one inclined and two adjacent horizontal sub-panels. Each panel half-wave consists of two inclined parts (inclined sub-panels) and one horizontal part (horizontal sub-panels) parallel to the longitudinal direction of the joist. Figure 14 shows the deformation distribution in the three sub-panels of the corrugated web (inclined and two horizontal sub-panels). The buckling deformation first appears in the inclined sub-panels and then propagates successively towards the two adjacent sub-panels. Buckling deformation is distributed between the three sub-panels in the diagonal direction and both senses. In contrast, the out-of-plane deformation of each sub-panel is different. The two horizontal sub-panels deform outwards, while the inclined sub-panel deforms inwards. As the load increased, further local buckling deformations occurred in several sub-panels, at different locations in the corrugated web. These deformations also occur in a diagonal direction and in both senses. The occurrence of two nearby interactive buckling deformations, in the same direction and opposite sense, creates a diagonal tension line. This tension line extends over the entire height of the strip, but before it reaches the flanges, a break occurs at the center of each tension line in the sub-panel of the corrugated web. This fracture mode obtained by numerical simulation corresponds to the fracture modes observed experimentally.

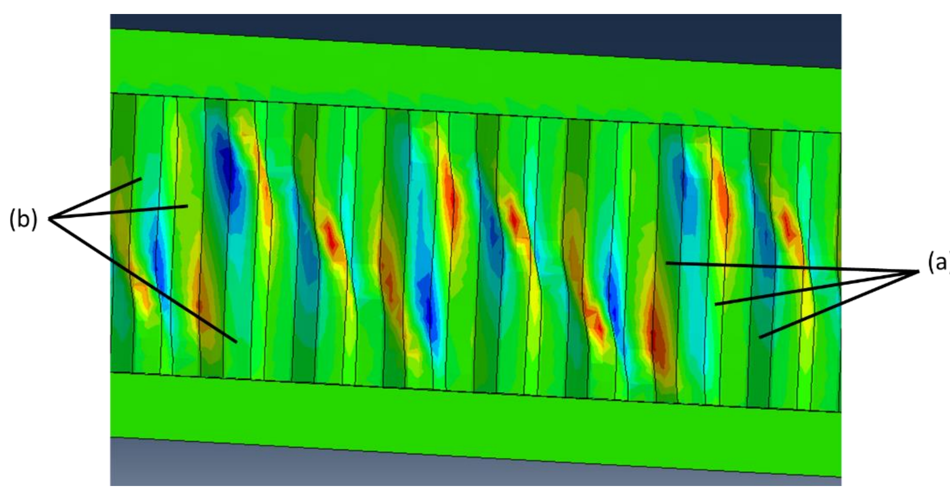


**Fig. 14.** Interactive buckling in the three sub-panels of the corrugated web: (a): Inclined sub-panels and (b): Horizontal sub-panels

As mentioned in the introduction, corrugated panels can have three failure modes under shear loading. In this study, the interactive buckling mode of failure was found in the corrugated web of the I-joist. This same behavior was also obtained in several previous studies. Wang *et al.* studied the shear failure mechanism of a large-scale corrugated steel web. They found interactive buckling behavior with similar diagonal tension lines, but the stage 3 plasticity behavior curve was much more developed. The use of steel as a base material allows the diagonal tension lines to extend over the entire height of the web, affecting the behavior of the flanges and beam stiffeners (Wang *et al.* 2023). In the present study, the effect of the tension line was limited to the web only, due to the small thickness and the weak properties of the corrugated panels used.

Investigation of the sensitivities of corrugated web properties on I-joist behavior has led to other interesting observations. Table 5 shows that the modulus of elasticity in the direction perpendicular to the corrugation has a negligible effect on the calculation of the joist stiffness ($EI_g$, $EI_s$, $K_s$), but a non-negligible effect on the maximum force obtained by numerical simulation. In the simulation, it was observed that as this modulus of elasticity decreases, the ultimate force $F_u$ is more easily reached, and the behavior of the joist passes from the elastic domain to final failure. Consequently, the modulus of elasticity is an important parameter in the buckling behavior of corrugated web.

Returning to the principle of the corrugated configuration in the plate, the corrugated shape enhances panel rigidity in the direction of corrugation, to the detriment of rigidity in the direction perpendicular to the corrugation. More specifically, when a corrugated panel is subjected to stress in the perpendicular direction of corrugation, it exhibits poor behavior. This is due to the low stiffness of the inclined subpanels due to their inclination with respect to the horizontal subpanels, which results in accordion-like behavior (Jiloul *et al.* 2023).

Consequently, the concentration of stresses and strains in the inclined subpanels obtained by numerical simulation is logical due to the low stiffness of these elements compared to the adjacent subpanels. It is only natural that these concentrations should be followed by buckling failure, given the small actual thickness of the corrugated panel (2 mm). It remains to be seen what type of buckling can occur. Each type depends on the corrugated web's geometric parameters and its mechanical properties. Local buckling depends mainly on the slenderness of the corrugated panel's horizontal or inclined sub-panels; and therefore, this type of buckling only occurs within the sub-panels. In contrast, the ratio of longitudinal and transverse moduli of elasticity is the controlling parameter in the case of global buckling because this occurs across several sub-panels. Consequently, the interactive buckling obtained in this study is analyzed as an interaction of these two types of buckling, controlled by both slenderness and modulus of elasticity ratio (Qui *et al.* 2022).

To improve the behavior of I-joists with corrugated web, it is necessary to increase the shear strength of the web. This shear resistance depends on the buckling mode introduced into the web. In previous studies of joists with corrugated web, several researchers have shown that global buckling and interactive buckling are unable to offer greater resistance than local buckling (Sebastiao and Papangelis 2023). Consequently, the geometries and properties of the joist web need to be modified so that the corrugated web is more sensitive to local buckling than to other types of buckling.

First of all, changing the geometry of the corrugations also can have a positive effect in achieving local buckling on the behavior of the corrugated web. These geometries include corrugation depth, radius, and height. With this increase, the corrugations become larger, and the number of corrugations required decreases (Luo and Edlund 1996; Chan *et al*. 2001; He *et al.* 2012). Secondly, increasing the actual thickness of the corrugated web can considerably improve the shear strength of the corrugated web. It can be achieved by manufacturing corrugated panels with more than two wood veneers, unlike the corrugated panels used in this study (Luo and Edlund 1996; He *et al.* 2012; Wu *et al.* 2020). Finally, the properties of the wood used in the manufacture of corrugated panels (species, density, quality, *etc.*) were also considered as an important parameter, so the use of stronger wood species improves the web's shear strength.

Finally, it would be interesting in the future to evaluate the structural performance of I-joists with corrugated web, but in the context of other types of mechanical tests, such as vibration tests. In addition, it would also be necessary to investigate the performance of joists with openings in the web for plumbing and ventilation ducts, as part of a future study.

In addition, the sensitivity study presented in this study focused solely on the properties of the corrugated web. However, the geometry of the corrugation has a very significant effect on the behavior of the joist in bending tests. It would, therefore, be interesting to carry out a sensitivity study to examine the effect of variations in corrugation depth, radius, and width on joist behavior. Such an approach would make it possible to determine the optimum corrugation configuration in the I-joist web.

## CONCLUSIONS

1. Numerical simulations of bending tests on I-joists with OSB web produced behavior curves and mechanical properties of the joists that agree well with the results of experimental bending tests. Only one exception was noted. The internal joist efforts determined in the long-span bending tests showed a non-negligible difference. This difference was attributed to the fact that the numerical model was idealized and did not take into account the singularities and defects of the wood as well as the flange or web butt joints present in the experimental model that had a non-negligible effect on the internal efforts determined.
2. The sensitivity study conducted on the bending test model of the I-joist with corrugated web showed that variation in the web elastic properties $E_2$ and $E_3$, $\nu_{12}$, $\nu_{13}$, $\nu_{23}$, $G_{13}$ and $G_{23}$ had a negligible effect on the elastic properties of the tested I-joist. In contrast, shear stiffness in the $G_{12}$ plane was the only dominant parameter in the elastic behavior of I-joists with corrugated web. Using the iterative method, this shear modulus was estimated at 1300 MPa to obtain a good correlation between experimental and numerical results.
3. The mode of shear rupture of the corrugated web found by numerical simulation was consistent with the failures obtained experimentally. This mode of rupture began to appear as localized interactive buckling in several sub-panels of the corrugated web. It was followed by the creation of diagonal tension lines and ended with a break in the center of the tension lines. In addition, the modulus of elasticity $E_2$ of the corrugated web had a considerable effect on the initiation and development of this mode of failure in joist bending tests.

## ACKNOWLEDGEMENTS

The authors are grateful to the Natural Sciences and Engineering Research Council of Canada for the financial support through its IRC and CRD programs (IRCPJ 461745-18 and RDCPJ 524504-18) as well as the industrial partners of the NSERC industrial chair on eco-responsible wood construction (CIRCERB).

## REFERENCES CITED

Abdalla, A. M. A., and Sekino, N. (2006). "Veneer strand flanged I-beam with MDF or particleboard as web material IV: Effect of web material types and flange density on the basic properties," *Journal of Wood Science* 52, 167-172. DOI: 10.1007/s10086-005-0745-4

Bai, X., Lee, A. W. C., Thompson, L. L., and Kosowsky D. V. (1999). "Finite element analysis of Moso bamboo-reinforced southern pine OSB composite beams," *Wood and Fiber Science* 31(4), 403-415.

Blanchet, P., Gendron, G., Cloutier, A., and Beauregard, R. (2005). "Numerical prediction of engineered wood flooring deformation," *Wood and Fiber Science* 37(3), 484-496.

Bodig, J., and Jayne, B. A. (1993). *Mechanics of Wood and Wood Composites*, Krieger Publishing Company, Malabar, FL, USA.

Chan, C. L., Khalid, Y. A., Sahari, B. B., and Hamouda, A. M. S. (2001). "Finite element analysis of corrugated web beams under bending," *Journal of Constructional Steel Research* 58(11), 1391-1406. DOI: 10.1016/S0143-974X(01)00075-X

Chen, G., Tan, C., Yang, W., Wu, J., Zhou T., Jiang, H., and Zhang, Y. (2021). "Wood I-joists with web holes and flange notches: A literature review," *Journal of Building Engineering* 38, article ID 102224. DOI: 10.1016/j.jobe.2021.102224

Driver, R. G., Abbas, H. H., and Sause, R. (2006). "Shear behavior of corrugated web bridge girders," *Journal of Structural Engineering* 132(2), 195-203. DOI: 10.1061/(ASCE)0733-9445(2006)132:2(195)

Elgaaly, M., Hamilton, R. W., and Seshadri, A. (1996). "Shear strength of beam with corrugated webs," *ASCE Journal of Structural Engineering* 122(4), 390-398. DOI: 10.1061/(ASCE)0733-9445(1996)122:4(390)

Fergus, D. (1979). *Effect of Web Voids and Stiffeners on the Structural Performance of Composite Beams*, Ph.D. Thesis, Purdue University, West Lafayette, IN, USA.

Grandmont, J. F., Cloutier, A., Gendron, G., and Desjardins, R. (2010). "Wood I-joist model sensitivity to oriented strandboard web mechanical properties," *Wood and Fiber Science* 42(3), 352-361.

Guan, Z. W., and Zhu, E. C. (2004). "Nonlinear finite element modeling of crack behavior in oriented strand board webbed wood I beams with openings," *Journal of Structural Engineering* 130(10), article 1562. DOI: 10.1061/(ASCE)0733-9445(2004)130:10(1562)

Guo, T., and Sause, R. (2014). "Analysis of local elastic shear buckling of trapezoidal corrugated steel webs," *Journal of Constructional Steel Research* 102, 59-71. DOI: 10.1016/j.jcsr.2014.06.006

He, J., Liu, Y., Chen, A., and Yoda, T. (2012). "Mechanical behavior and analysis of composite bridges with corrugated steel webs: State-of-the-art," *International Journal of Steel Structures* 12, 321-338. DOI: 10.1007/s13296-012-3003-9

Hughes, M. (2015). "Plywood and other veneer-based products," in: *Wood Composites*, M. Ansell (ed.), Woodhead Publishing, Sawston Cambridge, UK. DOI: 10.1016/B978-1-78242-454-3.00004-4

Jiloul, A., Blanchet, P., and Boudaud, C. (2023). "Mechanical characterization of corrugated wood-based panels and potential structural applications in a building," *Construction and Building Materials* 391, article ID 131896. DOI: 10.1016/j.conbuildmat.2023.131896

Jiloul, A., Blanchet, P., Boudaud, C., and Perez, C. (2024). "Structural evaluation of I-joists with corrugated panel web," *Construction and Building Materials* 442, article ID 137655. DOI: 10.1016/j.conbuildmat.2024.137655

Jiloul, A. (2024). D*éveloppement d'un Composite Structural de Nouvelle Génération*, Thèse de doctorat, Université Laval, Canada. https://hdl.handle.net/20.500.11794/143445

Li, Y., Zhang, W., Zhou, Q., and Qi, X. (2000). "Widera GEO. Buckling strength analysis of the web of a WCW H-beam: Part 2. Development and research on H-beams with wholly corrugated webs (WCW)," *Journal of Materials Processing Technology* 101(1), 115-128.

Liew, K. M., Peng, L. X., and Kitipornchai, S. (2007). "Nonlinear analysis of corrugated plates using a FSDT and a meshfree method," *Computer Methods in Applied Mechanics and Engineering* 196, 2358-2376. DOI: 10.1016/j.cma.2006.11.018

Luo, R., and Edlund, B. (1994). "Ultimate strength of girders with trapezoidally corrugated webs under patch loading," *Thin-Walled Structures* 24(1), 135-156.

Luo, R., and Edlund, B. (1996). "Shear capacity of plate girders with trapezoidally corrugated webs," *Thin-Walled Structures* 26(1), 19-44. DOI: 10.1016/0263-8231(96)00006-7

Ma, Y., Gong, Z., Zhao, L., Han, Y., and Wang, Y. (2014). "Finite element analysis of buckling of corrugated fiberboard," *The Open Mechanical Engineering Journal* 8, 257-263. DOI: 10.2174/1874155X01408010257

Moon, J., Yi, J., Choi, B. H., and Lee, H. E. (2009). "Shear strength and design of trapezoidally corrugated steel webs," *Journal of Constructional Steel Research* 65, 1198-1205. DOI: 10.1016/j.jcsr.2008.07.018

Morris, V., Gustafsson P. J., and Serrano E. (1995). *The Shear Strength of Light-Weight Beams with and Without a Hole- A Preliminary Study*, Workshop on Mechanical Properties of Panel Products, Watford, UK.

Nie, J. G., Zhu, L., Tao, M. X., and Tang, L. (2013). "Shear strength of trapezoidal corrugated steel webs," *Journal of Constructional Steel Research* 85, 105-115. DOI: 10.1016/j.jcsr.2013.02.012

Park, K. J., Jung, K., and Kim, Y. W. (2016). "Evaluation of homogenized effective properties for corrugated composite panels," *Composite Structures* 140, 644-654. DOI: 10.1016/j.compstruct.2016.01.002

Pathirana, S., and Qiao, P. (2020). "Elastic local buckling of periodic sinusoidal corrugated composite panels subjected to in-plane shear," *Thin-Walled Structures* 157, article ID 107134. DOI: 10.1016/j.tws.2020.107134

Peng, L. X., Liew, K. M., and Kitipornchai, S. (2007). "Analysis of stiffened corrugated plates based on the FSDT via the mesh-free method," *International Journal of Mechanical Sciences* 49(3), 364-378. DOI: 10.1016/j.ijmecsci.2006.08.018

Qiu, J., Zhao, Q., Wang, Z., and Yu, C. (2022). "Lateral behavior of trapezoidally corrugated wall plates in steel plate shear walls, Part 1: Elastic buckling," *Thin-Walled Structures* 174, article ID 109103. DOI: 10.1016/j.tws.2022.109104

Rouaz, I., and Bouzid, H. (2023). "Numerical evaluation of shear strength of CFS shear wall panel with OSB sheathing," *Structures* 57, article ID 105330. DOI: 10.1016/j.istruc.2023.105330

Sause, R., and Braxtan, T. R. (2011). "Shear strength of trapezoidal corrugated steel webs," *Journal of Constructional Steel Research* 67, 223-236. DOI: 10.1016/j.jcsr.2010.08.004

Sayed-Ahmed, E. Y. (2001). "Behavior of steel and (or) composite girders with corrugated steel webs," *Canadian Journal of Civil Engineering* 28(4), 656-672. DOI: 10.1139/cjce-28-4-656

Sebastiao, L., and Papangelis, J. (2023). "Elastic local shear buckling of beams with sinusoidal corrugated webs," *Structures* 54, 684-692. DOI: 10.1016/j.istruc.2023.05.080

Tang, R. C., and Leichti, R. J. (1984). "Manufacturing composite wood I-beams by using small diameter trees and its engineering performance," in: *Symposium of Utilization of Medium and Small Diameter Trees*, Taichung, Taiwan, Republic of China. (in Chinese)

Wang, S., He, J., and Liu, Y. (2019). "Shear behavior of steel I-girder with stiffened corrugated web, Part I: Experimental study," *Thin-Walled Structures* 147, article ID 106025. DOI: 10.1016/j.tws.2019.02.023

Wang, S., Zhang, K., Zhang, Y., and Liu, Y. (2023). "Shear failure mechanism of local buckling-dominated large-scale corrugated steel web," *Thin-Walled Structures* 182, article ID 110279. DOI: 10.1016/j.tws.2022.110279

Wu, C. S., Hassanein, M. F., Deng, H., Zhang, Y. M., and Shao, Y. B. (2020). "Shear buckling response of S690 steel plate girders with corrugated webs," *Thin-Walled Structures* 157, article ID 107015. DOI: 10.1016/j.tws.2020.107015

Yi, J. W., Gil, H., Youm, H., and Lee, H. E. (2008). "Interactive shear buckling of trapezoidally corrugated steel webs," *Engineering Structures* 30, 1659-1666. DOI: 10.1016/j.engstruct.2007.11.009

Zhang, W., Li, Y., Zhou, Q., Qi, X., and Widera, G. E. O. (2000a). "Optimization of the structure of an H-beam with either a flat or a corrugated web. Part 3: Development and research on H-beams with wholly corrugated webs," *Journal of Materials Processing Technology* 101(1), 119-123.

Zhang, W., Zhou, Q., Li, Y., Cai, Z., and Widera, G. E. O. (2000b). "Hot rolling technique and profile design of toothshape rolls. Part 1: Development and research on H-beams with wholly corrugated webs," *Journal of Materials Processing Technology* 101(1), 110-124.

Zhu, E. (2003). *Modelling the Structural Behavior of OSB Webbed Timber I-Beams*, Ph.D. Thesis, University of Brighton, Brighton, UK.

Zhu, E. C., Guan, Z. W., Pepe, D. J., and Rodd, P. D. (2007). "Effect of openings on oriented strand board webbed wood I-joists," *Journal of Structural Engineering* 133(1), article 145. DOI: 10.1061/(ASCE)0733-9445(2007)133:1(145)

Zhu, E. C., Guan, Z. W., Rodd, P. D., and Pope, D. J. (2005a). "A constitutive model for OSB and its application in finite element analysis," *European Journal of Wood and Wood Products* 63, 87-93. DOI: 10.1007/s00107-004-0513-y

Zhu, E. C., Guan, Z. W., Rodd, P. D., and Pope, D. J. (2005b). "Finite element modelling of OSB webbed timber I-beams with interactions between openings," *Advances in Engineering Software* 36(11-12), 797-805. DOI: 10.1016/j.advengsoft.2005.03.027

Article submitted July 29, 2024: Peer review completed: October 26, 2024; Revised version received: November 8, 2024; Accepted: November 9, 2024; Published: November 21, 2024.
DOI: 10.15376/biores.20.1.737-764